



中国科学院大学
University of Chinese Academy of Sciences

博士学位论文

亚非季风区夏季降水预估的不确定性与观测约束研究

作者姓名: 陈梓明

指导教师: 周天军 研究员 中国科学院大气物理研究所

学位类别: 理学博士

学科专业: 气象学

培养单位: 中国科学院大气物理研究所

2022 年 6 月

**Projection Uncertainty and Observational Constraint on the
Summer Precipitation over the Afro-Asian Monsoon Region**

**A dissertation submitted to
University of Chinese Academy of Sciences
in partial fulfillment of the requirement
for the degree of
Doctor of Philosophy
in Meteorology**

**By
Chen Ziming
Dissertation Supervisor : Professor Zhou Tianjun**

Institute of Atmospheric Physics, Chinese Academy of Sciences

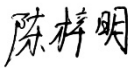
June 2022

谨以此论文献给我的导师以及帮过我的所有人

——陈梓明

中国科学院大学
研究生学位论文原创性声明

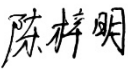
本人郑重声明：所呈交的学位论文是本人在导师的指导下独立进行研究工作所取得的成果。尽我所知，除文中已经注明引用的内容外，本论文不包含任何其他个人或集体已经发表或撰写过的研究成果。对论文所涉及的研究工作做出贡献的其他个人和集体，均已在文中以明确方式标明或致谢。


作者签名： 
日 期：2022 年 6 月

中国科学院大学
学位论文授权使用声明

本人完全了解并同意遵守中国科学院有关保存和使用学位论文的规定，即中国科学院有权保留送交学位论文的副本，允许该论文被查阅，可以按照学术研究公开原则和保护知识产权的原则公布该论文的全部或部分内容，可以采用影印、缩印或其他复制手段保存、汇编本学位论文。

涉密及延迟公开的学位论文在解密或延迟期后适用本声明。

作者签名： 
日 期：2022 年 6 月

导师签名： 
日 期：2022 年 6 月

摘要

亚非季风由东亚、南亚和西非季风组成，它是全球季风系统的重要组成部分。一方面，亚非季风区内干湿季转换明显，降水主要集中在夏季，是该地区淡水资源的主要来源；另一方面，季风区内人口稠密，季风活动异常对经济和社会影响较大。准确的气候预估结果是开展气候变化影响和适应的重要基础。

当前的气候模式对未来季风降水的预估结果中存在不确定性。气候预估包括近期（2021~2040）、中期（2041~2060）和远期（2081~2100）三个特征时间段，不同预估时段内的预估结果的不确定性来源不同。本文针对近期和中远期的预估问题，借助可靠的观测资料，对未来预估结果进行约束校正，以提高未来预估结果的可信度；并且基于扰动参数的数值试验，理解不同模式参数对未来预估结果的影响。

本文首先评估和比较了 CMIP5 和 CMIP6 的气候模式对季风降水及相关物理过程的模拟技巧，并分析模拟偏差的成因。其次，利用参加第六次耦合模式比较计划（CMIP6）的多模式集合，理解和预估全球陆地季风区的降水在不同时段的未来变化。第三，由于不同预估时段内，不确定性的来源不同，本文有针对性地对不同时段降水预估结果进行观测约束，重点关注对升温响应最强烈的亚非季风区；并基于观测约束后的降水预估结果，估计当地未来潜在水资源的变化及其风险。亚非季风区涵盖众多发展中国家，且人口约占全球的三分之一，更可靠的降水和水资源预估结果，对于该地区开展气候变化应对工作具有重要的参考价值。

本文的主要结论如下：

一、CMIP6 模式对全球季风系统具有更高的模拟技巧，半球间的热力差异以及湿静力能的经向梯度模拟改进是重要原因

以 1979 年以来，多套降水观测资料以及再分析数据为基准，评估 CMIP5 和 CMIP6 集合的 20 个相同的气候模式对全球季风的模拟技巧，并从能量的角度理解偏差的成因。结果表明大部分 CMIP6 的模式对全球季风区的降水以及相关的物理过程的模拟技巧，都比 CMIP5 的模式更高，综合的技巧评分普遍超过 0.7。其中 CMIP6 模式中，北半球季风区的夏季降水的干偏差比 CMIP5 显著减少，两

代模式的多模式集合平均的均方根偏差分别为 1.66 mm day^{-1} 和 1.85 mm day^{-1} 。这对冬夏季模态的降水、季风降水的强度以及季风区的面积范围的技巧提高起主要贡献。降水干偏差显著减少主要与大气温度的分布和能量的经向输送的模拟技巧提高有关。在北半球夏季, CMIP6 模拟的地表入射长波辐射, 以及输入北半球的能量都比 CMIP5 更接近观测, 半球间的热力差异以及湿静力能的经向梯度也都更接近观测, 因此北半球的夏季风环流以及降水的偏差减少。相比之下, 南半球季风区的夏季降水的模拟技巧提高不明显, 总体以湿偏差为主, 均方根偏差为 1.85 mm day^{-1} , 与 CMIP5 相当 (1.77 mm day^{-1}), 因为大气层顶入射的长波辐射和地表入射的短波辐射的正偏差在两代模式间的差异不明显。但从全球季风系统的角度上看, CMIP6 的模拟技巧普遍更高。

二、热力(动力)过程主导未来预估中全球季风降水的增多(不确定性)

基于 CMIP6 的多模式集合, 在不同排放情景下的预估试验数据, 揭示研究了全球陆地季风区的夏季降水的未来变化和预估的不确定性, 以及动力和热力过程的贡献。结果显示, 未来预估中全球陆地季风区的夏季降水普遍增多。近期预估中 (2021~2040), 降水增多 $0.96\% \sim 1.76\%$, 在情景间的差异较小; 远期预估中 (2080~2099), 降水增幅随排放情景加强而增强, 在 SSP1-2.6、SSP2-4.5、SSP3-7.0 和 SSP5-8.5 情景下, 分别增多 2.54% ($0.32\% \sim 4.76\%$, $10^{\text{th}} \sim 90^{\text{th}}$ 百分位的范围)、 3.52% ($0.47\% \sim 6.58\%$)、 3.51% ($-1.46\% \sim 8.49\%$) 和 5.75% ($-0.17\% \sim 11.68\%$)。区域尺度上, 亚非季风区的降水增幅最强, 在近期预估增多 $1.89\% \sim 3.97\%$, 远期预估分别增多 5.67% ($0.92\% \sim 10.42\%$)、 7.69% ($1.40\% \sim 13.99\%$)、 9.55% ($0.52\% \sim 18.56\%$) 和 13.77% ($2.97\% \sim 24.57\%$)。降水的增多主要由变暖背景下大气中水汽含量增多(热力项)主导, 相反垂直环流减弱(动力项)则部分抵消水汽增多的贡献。除了 SSP1-2.6 情景下, 预估的不确定性随时间而增大, 在 SSP5-8.5 情景下, 预估的不确定性最大, 约 11.85% 。子季风区内预估的不确定性比全球陆地季风区的更大。降水预估的不确定性, 主要由环流变化的不确定性贡献。与全球陆地季风区和其他子季风区不同, 亚非季风区的夏季降水的预估不确定性除了受环流变化的影响以外, 还与全球平均升温的预估不确定性紧密关联。

三、针对近期气候预估问题, 基于观测中北大西洋(AMO)和热带太平洋(IPO)海温年代际变率与季风降水的关系建立一个统计模型, 通过约束 AMO 和 IPO

的位相，发现亚非季风区的降水变化将呈现负异常

基于观测中 AMO 和 IPO 的位相转换，借助多套单一模式的大样本集合的历史模拟和 RCP8.5 情景下的模拟结果，建立基于物理的统计模型（PS 模型），来约束近期预估中（2021~2040），亚非季风区夏季降水的变化。结果显示，基于观测中的 AMO 和 IPO 指数，PS 模型能合理再现 1960~1990 年间亚非季风区的降水减少，以及 1990s 中后期至今的降水恢复，模型与观测序列之间的相关系数为 0.74 ($p < 0.001$)；局地尺度上 PS 模型具有显著的回报技巧，异常相关系数和均方技巧评分普遍超过 0.5 和 0.3，不同时段内降水变化趋势在模型和观测之间的空间相关系数均超过 0.54。从七套大样本集合的 286 个样本成员中，分别挑选 AMO 指数和 IPO 指数最接近观测的 10 个样本成员，来约束当前和近期预估中的降水异常。约束后的降水异常基本与观测一致 ($r = 0.73$, $p < 0.001$)，样本间的差异显著减少；在 RCP8.5 情景下的近期预估，约束后亚非季风区的夏季降水普遍呈现负异常（区域平均约为 -3.01% ($-5.56\% \sim -0.10\%$)），相比之下约束前的预估结果为正异常 (1.79% ($-3.89\% \sim 7.85\%$))，因此约束后的不确定性范围仅为约束前的 46%。约束后，降水减少的概率从约束前的 19% 提高至 78%。约束后预估结果的信噪比普遍提高，超过 77% 的区域内，预估结果的信噪比超过 1。借助约束后的降水，进一步约束当地潜在水资源的未来变化（定义为总径流量的变化）。未来潜在水资源显著减少的面积约为 48%，均超过原始预估的结果（29%~45%）。其中东亚季风区内受影响的面积最大（约 37%）。

四、针对中远期气候预估问题，基于气候敏感性和半球间温差的关系，设计了基于观测数据的萌现约束方法，约束预估的亚非季风区降水和潜在可用水资源的增幅显著减弱

基于亚非季风区降水预估的不确定性与当前半球间升温幅度差异（ITC）的模拟偏差的物理联系，采用多套可靠的温度观测资料和 CMIP6 模式在 SSP5-8.5 情景下的预估试验的数据，对中远期气候预估（2050~2099），亚非季风区夏季降水的变化进行约束。结果显示，平衡态气候敏感性（ECS）越高的模式，当前和未来预估中 ITC 的增幅越强，导致亚非季风区夏季风环流和水汽通量越强，夏季降水越多。基于当前观测中的 ITC 趋势，约束亚非季风区的夏季降水，约束后未来降水的增幅约为 10%，比原始的预估结果减弱约 30%，预估的不确定性减少约

10%。其中在西非和东亚季风区，约束效果最为明显，约束后比约束前分别减弱约 51%和 30%。进一步基于约束后的降水预估结果，约束潜在水资源的未来变化。约束后，未来降水或潜在水资源显著增多的面积范围，仅为约束前的 57%和 66%。在区域尺度上，东亚（西非）季风区的降水（潜在水资源）的空间分布受约束的影响最大，未来出现显著增多的面积占比仅为约束前的 37%（55%）。

五、基于参数扰动集合试验，发现副热带下沉区的云量和云水含量是影响未来半球间升温幅度差异的主要因子

为了探究调控 ITC 预估的不确定性的关键模式参数及其背后的物理过程，基于 HadGEM3-GC3.05 在历史模拟和 RCP8.5 情景下扰动参数的大样本集合的数据，以及广义线性模型，揭示了四个与 ITC 预估的不确定性显著相关的模式参数化方案的参数，包括对流参数化方案中控制凝结物含量的参数 `qlmin`、云宏观物理参数化方案中控制冰雪颗粒宽度的参数 `ice_width`、云微物理参数化方案中控制冰晶粒子纵横比的参数 `ar` 和边界层湍流参数化方案中控制中性混合长的参数 `par_mezla`。上述四个潜在参数的相对贡献分别是 16%、10%、7%和 8%。其中参数 `qlmin` 的相对贡献最大，其调控 ITC 预估的不确定性的主要物理过程如下：参数 `qlmin` 越大的样本成员里，当前热带的高云云量越多，外逸长波辐射越少，热带对流层的气温越高；由于预估中哈德莱环流上升支和下沉区分别将会收缩和变宽，在北半球夏季，预估中副热带的云量和云凝结水含量的减少幅度更强，局地的短波云辐射反馈更强；在其主导下，净云辐射反馈更强，因此北半球副热带地区升温幅度更强；相反在南半球，由于副热带地区的云量和云水含量增多或者变化不显著，因此局地升温幅度偏弱或者变化不显著。在参数 `qlmin` 偏大的样本成员中，北半球副热带地区的升温幅度比南半球更强，最终导致 ITC 增大。

关键词：全球季风，亚非季风，观测约束，未来预估，潜在水资源

Abstract

The Afro-Asian summer monsoon (AfroASM), a major component of the global monsoon system, consists of East Asian, South Asian and West African monsoon regions. On the one hand, given that the precipitation mainly occurs in summer, the AfroASM features a distinct wet-dry season contrast. The changes or variabilities of precipitation would directly affect local water resource. On the other hand, the AfroASM sustains billions of people living in many developing countries, which are vulnerable to climate change. Thus, a reliable projection results is of importance to the mitigation and adaptation strategies of climate change.

Given that, this dissertation mainly focuses on the future changes of AfroASM precipitation. Since the future increase in AfroASM precipitation projected by current state-of-the-art climate models exhibits a large spread, viz projection uncertainty, we aim to constrain and narrow the projection uncertainty to improve the reliability of future projection results, based on the sources of projection uncertainty in different future projection terms, and the physical linkage between the projection uncertainty and present-day model biases. In addition, we explore the impact of perturbed model parameters on the future projection using the perturbed parameter ensemble (PPE).

We first evaluate the simulation skill of state-of-the-art climate models to the monsoon precipitation and related physical processes from the Coupled Model Intercomparison Project Phase 5 (CMIP5) and Phase 6 (CMIP6), and investigate the causes of model biases. In addition, based on 30 models from the CMIP6, we investigate the future changes in global land monsoon precipitation under different CMIP6 scenarios in different periods, and reveal the mechanisms for the changes of precipitation and the sources of projection uncertainty. Next, we constrain and narrow the projection uncertainty of AfroASM precipitation specifically in different projection terms. Using the constrained projection of precipitation, we evaluate the projected changes and potential exposure of potential water availability. These issues are of vital

importance for future water management and planning, mitigation and adaptation strategies, sustainable development and carbon neutralization. The main conclusions are summarized as follows.

1. A higher simulation skill of CMIP6 models to global monsoon system due to a higher skill of interhemispheric thermal contrast and meridional moist static energy gradient

Based on multiple reliable observational and reanalysis datasets, we evaluate the simulation skills of 20 climate models in CMIP5 and CMIP6 ensemble to the global monsoon system, and investigate the causes of model biases from the perspective of energy budget. The results show that most models in CMIP6 ensemble have a higher skill than that of CMIP5 version. The comprehensive skill scores of CMIP6 models exceed 0.7. The dry biases in the Northern hemisphere summer monsoon (NHSM) precipitation decrease significantly in CMIP6 ensemble ($\text{RMSE} = 1.66 \text{ mm day}^{-1}$) compared to CMIP5 ensemble ($\text{RMSE} = 1.85 \text{ mm day}^{-1}$), which make the main contribution to a higher skill in simulating the solstitial mode of precipitation, monsoon intensity and the monsoon regions. The lower dry biases in NHSM precipitation are related to the higher skill in simulating the atmospheric temperature pattern and the meridional transport of atmospheric energy. In the boreal summer, the negative biases of the surface downward longwave radiation and the northward transport of atmospheric energy in CMIP6 are lower than that of CMIP5. So CMIP6 models simulate a more realistic interhemispheric thermal contrast (ITC) and meridional gradient of moist static energy (MSE), and the dry biases of NHSM precipitation is lower. In contrast, the improvement of simulation skill of Southern hemisphere summer monsoon (SHSM) precipitation is not significant in CMIP6 ($\text{RMSE} = 1.85 \text{ mm day}^{-1}$) compared with CMIP5 ($\text{RMSE} = 1.77 \text{ mm day}^{-1}$), since the positive biases of top-of-atmosphere downward radiation and surface downward shortwave radiation in CMIP6 are higher than that in CMIP5. In general, the simulation skill of CMIP6 models to the global monsoon system is higher than that of CMIP5.

2. The projected changes and uncertainty of monsoon precipitation are dominated by the thermodynamic and dynamic responses, respectively

The future changes in global land monsoon summer precipitation and the sources of projection uncertainty under four scenarios are investigated using the CMIP6 models. The global land monsoon precipitation is projected to increase by 1.76% (0.19%~3.33% for the 10th-90th ensemble range) and 2.54% (0.32%~4.76%), 1.33% (−0.64%~3.30%) and 3.52% (0.47%~6.58%), 0.96% (−1.08%~2.99%) and 3.51% (−1.46%~8.49%), 1.71% (−0.67%~4.10%) and 5.75% (−0.17%~11.68%) in the near- and long-term projections under Shared Socioeconomic Pathway (SSP) 1-2.6, SSP2-4.5, SSP3-7.0, and SSP5-8.5 scenarios, respectively. In the regional scale, the enhancement of AfroASM precipitation is larger than that over global and other submonsoon regions, by 3.30% (−0.51%~7.12%) and 5.67% (0.92%~10.42%), 2.76% (−0.53%~6.05%) and 7.69% (1.40%~13.99%), 1.89% (−2.13%~5.91%) and 9.55% (0.52%~18.56%), 3.97% (−0.48%~8.41%) and 13.77% (2.97%~24.57%), respectively. The enhancement is caused by thermodynamic response associated with the increase of water vapor, but partly offset by dynamic response due to weakened circulation. The projection uncertainty increases with projection terms except for SSP1-2.6 scenario, and the uncertainty is the largest in SSP5-8.5 long-term projection. The uncertainty of submonsoon precipitation is larger than that in global land monsoon precipitation. The projection uncertainty of precipitation over global land monsoon and submonsoon regions arises from the projection spread of circulation changes. The projection uncertainty of AfroASM precipitation is significantly correlated with the projection uncertainty of global surface air temperature (GSAT) warming, which is different from that over global and other submonsoon regions.

3. A negative anomaly of AfroASM precipitation after constraining the phase transition of AMO and IPO in the near-term climate projection

Based on the observed phase transition of Atlantic multidecadal oscillation (AMO) and interdecadal Pacific oscillation (IPO), using the outputs of multi-model large ensemble archive (MMLEA), we set up a physical-based statistical model (PS model) and constrain the near-term projection of AfroASM precipitation for the period of 2021~2040. The results show that the PS model can reasonably reproduce the decadal variability of AfroASM precipitation, including the drying tendency for the period of

1960~1990 and the recovery of precipitation since the late 1990s, with a high correlation coefficient of 0.74 ($p < 0.001$) between PS model and observation. In the local scale, a significant hindcast skill of PS model can be seen, with Pearson anomaly correlation coefficient (ACC) and mean squared skill score (MSSS) exceeding 0.5 and 0.3, respectively. In addition, the PS model can reasonably reproduce the spatial pattern of 20-year trend of summer precipitation, with pattern correlation coefficient (PCC) higher than 0.54 in different time periods. By selecting top 10 ensemble members in which the phase transition of AMO and IPO indexes is similar with that in observation, respectively, from the 287 ensemble members of MMLEA, we constrain the precipitation anomaly in present day and near-term projection. The decadal variability of constrained AfroASM precipitation anomaly is similar with that in observation, with a high correlation coefficient of 0.73 ($p < 0.001$). In addition, the inter-member spread after constraint is narrowed significantly. In the near term, a negative anomaly (-3.01% ($-5.56\% \sim -0.10\%$)) can be seen over AfroASM region after constraint, which is lower than that of raw projection (1.79% ($-3.89\% \sim 7.85\%$)). It suggests that the constrained projection uncertainty is 46% of that of raw projection. In addition, the signal-to-noise ratio generally exceeds 1 in the constrained projection. By using the constrained projection of AfroASM precipitation, we estimate the future changes of potential water availability which is defined by the changes of runoff. The land fraction that experiences a significant decrease is about 48%, which is higher than that of raw projection by seven large ensembles (29%~45%). Regionally, the land fraction in East Asian monsoon region is highest among three submonsoon regions by about 37%.

4. Emergent constraint indicates a less increase of AfroASM precipitation and potential water availability in the mid- and long-term projections

Since the projection uncertainty of AfroASM precipitation in the midterm and long term is related to present-day ITC, we constrain the mid- and long-term projections of AfroASM precipitation for the period of 2050~2099, using multiple reliable observational datasets and the output of projection experiment under SSP5-8.5 scenario from CMIP6 ensemble, based on the emergent constraint technique. The inter-model spread of ITC is associated with that of global mean warming rate under a specific

radiative forcing, i.e., the equilibrium climate sensitivity (ECS). Climate models with a larger ECS show a larger ITC in both the historical and future periods. A larger increase of ITC would lead to a stronger enhancement of low-level cross-equatorial flow, and thereby project more precipitation over AfroASM precipitation. Using present-day ITC trend in the observation, the mid- and long-term projection of AfroASM precipitation is constrained. The emergent constraint indicates that the constrained AfroASM precipitation increases by about 10% relative to present-day climate, which is only 70% of raw projection. In addition, the projection uncertainty is narrowed by about 10%. Regionally, a pronounced reduction can be seen in West African and East Asian monsoon regions, which is only 49% and 70% of the raw projection. By using the constrained projection of precipitation, we further investigate the impacts of the constrained projection on the potential water availability. The fractions of land area that will experience a significant increase of precipitation and potential water availability are about 57% and 66% of the raw projection, respectively. Regionally, the land fraction that will experience a significant increase of precipitation (potential water availability) over East Asian (West African) monsoon region are only about 37% (55%) of that of raw projection.

5. The mass of cloud condensed water is a dominant factor which affect the projection uncertainty of interhemispheric thermal contrast based on the PPE experiment

To investigate the key physical parameters and mechanism behind of modulating the projection uncertainty of ITC changes, we analysis the output of perturbed parameter ensemble (PPE) experiment of HadGEM3-GC3.05. The PPE experiments include historical simulation for the period of 1900-2005 and future projection run under RCP8.5 scenario for the period of 2006-2100. The results show that the projection uncertainty of ITC is significantly correlated with four potential parameters, including the parameter of minimum critical cloud condensate (ql_{min}) from convection scheme, the parameter of ice width (ice_width) from cloud/cloud radiation scheme, the parameter of aspect ratio of ice particles (ar) from cloud microphysics scheme, and the parameter of neutral mixing length (par_mezcla) from boundary layer scheme. Based

on the generalized linear model, the relative contribution of above potential parameters to the inter-member variance of ITC projection account for 16%, 10%, 7% and 8%, respectively, among which the parameter ql_{min} make the largest contribution. An ensemble member with a larger ql_{min} tends to simulate a warmer tropical troposphere for a larger amount of high cloud. Given that the ascending (descending) branch of Hadley Circulation over tropics and subtropics will be tighter (wider) in the future projection, the projected decrease of subtropical cloud fraction and condense water pathway in the Northern hemisphere will be larger in the boreal summer in the ensemble member with a larger ql_{min} . The local shortwave cloud radiation positive feedback in the Northern hemisphere, which dominates the net cloud radiation feedback, will be larger. Finally, the surface warming in the projection in the Northern subtropics will be larger in the ensemble member with a larger ql_{min} , and vice versa for Southern subtropics. Thus, a larger ITC can be seen.

Key words: Global monsoon, Afro-Asian monsoon, Observational constraint, Future projection, Potential water availability

目 录

| | |
|--|----|
| 第一章 绪论 | 1 |
| 1.1 选题依据和研究意义 | 1 |
| 1.2 国内外相关的研究进展 | 3 |
| 1.2.1 全球季风降水的历史变化..... | 3 |
| 1.2.2 亚非季风区降水的历史变化..... | 5 |
| 1.2.3 未来预估中季风降水的变化..... | 9 |
| 1.2.4 影响气候变化的不确定性的关键因子..... | 11 |
| 1.2.5 自然内部变率对季风降水在近期预估的影响..... | 13 |
| 1.2.6 模式不确定性对季风降水预估的影响..... | 14 |
| 1.3 论文研究内容 | 18 |
| 1.3.1 拟解决的科学问题..... | 18 |
| 1.3.2 论文章节安排..... | 19 |
| 第二章 季风降水的模拟评估 | 21 |
| 2.1 引言 | 21 |
| 2.2 数据和方法 | 22 |
| 2.2.1 观测资料..... | 22 |
| 2.2.2 模式数据..... | 23 |
| 2.2.3 方法..... | 24 |
| 2.3 结果分析 | 25 |
| 2.3.1 CMIP5 和 CMIP6 模式对全球季风区的气候态的模拟技巧 | 25 |
| 2.3.2 CMIP6 的模拟技巧的提高与全球温度分布的技巧提高相关联 | 29 |
| 2.3.3 CMIP6 模式对全球季风的综合模拟技巧比 CMIP5 模式更高 | 36 |
| 2.4 总结和讨论 | 38 |
| 2.4.1 小结..... | 38 |
| 2.4.2 讨论..... | 39 |
| 第三章 季风降水变化的预估及其不确定性与动力热力过程的关系 .. | |
| | 41 |
| 3.1 引言 | 41 |